

Steady Gravity-Capillary Waves on Deep Water—

II. Numerical Results for Finite Amplitude

By B. Chen and P. G. Saffman

Finite amplitude capillary-gravity waves of permanent form on deep water are studied numerically. Bifurcation and limit lines are calculated. Pure and combination waves are continued to maximum amplitude. It is found that the height is limited in all cases by the surface enclosing one or more bubbles.

1. Introduction

In Part I ([2], hereafter referred to as I) we discussed the properties of weakly nonlinear capillary-gravity waves of permanent form. It was shown that there exist different types of solutions which could conveniently be categorized as pure and combination waves, at least when their amplitude is small. A pure wave of degree or class N has the property that the N th harmonic is dominant and only the higher harmonics of this fundamental mode are nonzero. In a combination (M, N) wave, two harmonics are of equal importance, the M th and N th, where M and N can be supposed coprime without loss of generality, and the other harmonics are much smaller. It was shown that bifurcation loci or limit lines exist at which a continuous family of pure waves can bifurcate or change into a combination wave and vice versa. A corollary of this result is that steady capillary-gravity waves are not in general unique, in the sense that given the height of the wave h (defined as the vertical distance between the highest crest and lowest trough) and the wavelength λ (defined as the shortest period), there exists more than one solution.

Special cases of the corollary have been known for some time. Wilton [10] demonstrated two types of weakly nonlinear wave for $\lambda = 2\pi(2T/\rho g)^{1/2}$, where T is the surface tension, ρ the density of the liquid and g the acceleration due to

Address for correspondence: Professor P. G. Saffman, Firestone Building, California Institute of Technology, Pasadena, CA 91125.

gravity. (The density of the upper fluid, usually air, is neglected.) Pierson and Fife [9] discussed solutions for neighboring values of λ . Nayfeh [8] found three solutions for wavelengths close to $\lambda = 2\pi(3T/\rho g)^{1/2}$. Recently Chen and Saffman [3] have demonstrated that gravity waves ($T=0$) are also not unique when their amplitude is sufficiently large.

The purpose of the present paper is to extend some of the results obtained in I for waves of small amplitude to waves of finite amplitude. The structure of capillary-gravity waves appears to be extremely rich, and our contribution is far from being an exhaustive study. We shall concentrate on extending to finite amplitude some of the bifurcation loci examined in I and also investigating limiting waves of greatest height. The stability of the waves is a matter for further study.

2. Numerical procedure

The equations that are solved and the numerical method have already been described in I (Secs. 1 and 10) and [3, Sec. 4]. We repeat here only the essence of the approach.

In a coordinate system moving with the wave, the profile in a window of length L can be written parametrically

$$\frac{2\pi x}{L} = \zeta + \sum_1^{\infty} \frac{A_n}{n} \sin n\zeta, \quad \frac{2\pi y}{L} = \sum_1^{\infty} \frac{A_n}{n} (\cos n\zeta - 1), \quad 0 \leq \zeta \leq 2\pi. \quad (2.1)$$

The wave is taken to be steady, inviscid, irrotational, progressive and one dimensional. It is also assumed to be symmetrical about the origin, which is a crest or trough. (The existence of solutions nonsymmetrical about all crests and troughs remains an open question.) Bernoulli's equation can be written

$$q^2 + 2gy - \frac{2T}{R} = c^2(1 - b), \quad (2.2)$$

where c is the wave speed, R is the radius of curvature, and

$$q^2 = \frac{c^2}{L^2} \left[\left(\frac{\partial x}{\partial \zeta} \right)^2 + \left(\frac{\partial y}{\partial \zeta} \right)^2 \right]^{-1} \quad (2.3)$$

is the surface speed of the fluid. The parameter b can be used as a measure of the wave amplitude, provided $g \neq 0$, since it can be shown by the method of Lamb [7, p. 420] that

$$2g\bar{y} = -bc^2, \quad (2.4)$$

where the overbar denotes the average value over the period. Substitution of (2.1) into (2.3) gives an infinite number of equations for the A_n ($n=1, 2, 3, \dots$), b and c^2 [see I, Eq. (1.7)]. Specification of the wave height or an equivalent parameter completes the system of equations.

A numerical approximation is constructed by solving a truncated version, obtained as described in I (Sec. 10), by Newton's method. A continuous solution branch can then be found by continuing in the waveheight or equivalent variable, or in a physical parameter such as surface tension. Keller's [6] method of pseudo arclength continuation handles without trouble limit points and simple bifurcation points, at which the determinant of the Jacobian matrix has a simple zero (see [3, Secs. 3, 4]).

The method of Fourier series truncation was completely adequate for the calculation of capillary-gravity waves up to waves of greatest height, but some of the results were checked using the vortex sheet integrodifferential approach (I, Sec. 10; [3]), which is necessary for gravity waves of large amplitude because of the incipient cusp, which causes slow decay of the Fourier coefficients. As will be seen, capillary-gravity waves are limited in height by the surface crossing itself, as for capillary waves with $g=0$ [5], but the surface remains smooth and the rate of decay of the Fourier coefficients is not significantly affected as the limiting wave is approached.

The coefficients A_n are dimensionless. Dimensionless groups involving the surface tension which are convenient for presentation of the results are

$$\kappa = \frac{4\pi^2 T}{gL^2} \quad \text{or} \quad \tilde{\kappa} = \frac{\kappa}{1+\kappa}. \quad (2.5)$$

The latter is useful for the capillary wave limit, $g \rightarrow 0$. In the actual calculations, the values $g=1$, $L=2\pi$ were employed. Continuation along a solution branch was carried out either in an amplitude parameter ϵ that was either b or a linear combination of Fourier coefficients, or in the surface tension variable κ . Full details of the numerical method are given in [1].

All numerical calculations were carried out on the CDC STAR 100.

3. The finite amplitude $2 \rightarrow 1$ and $2 \rightarrow 3$ bifurcations

In I, Sec. 4, it was shown that a weakly nonlinear pure wave of degree 2 bifurcates into a combination $(2, 1)$ wave when

$$A_2 \doteq \frac{4}{3}\kappa - \frac{2}{3} \doteq 2\left(\tilde{\kappa} - \frac{1}{3}\right), \quad \left|\kappa - \frac{1}{2}\right| \ll 1. \quad (3.1)$$

In physical variables, this condition is equivalent to

$$\frac{h}{\lambda} = \frac{4}{3\pi} \left| \frac{\pi^2 T}{g\lambda^2} - \frac{1}{2} \right| \quad (3.2)$$

as the condition for a pure wave of height h and wavelength λ to bifurcate by the addition of a subharmonic of wavelength 2λ .

To extend the bifurcation curve (3.1) to waves of finite amplitude, we employed continuation alternately in ϵ and κ . Starting for $\kappa > \frac{1}{2}$ with a small amplitude pure wave of degree 2 with $A_2 > 0$, we increased the amplitude until a

change of sign of the determinant of the Jacobian matrix occurred, indicating that the solution branch went through a critical point. Since it was easily seen that this was not a limit point, as all variables were changing monotonically, a crossing of the bifurcation curve had taken place. A continuation increasing κ was then carried out until the bifurcation curve was crossed again. The process was continued, and in this way a rough profile of the bifurcation curve was obtained. The curve ended at $\kappa = 1.342$, $A_2 = 0.77$, $h/\lambda = 0.48$, where the surface crossed itself. The unphysical nature of the solutions for larger amplitudes was not marked by any singularity in the equations for the Fourier components, which could be calculated without difficulty for unphysical solutions.

Note the conclusion that for $\kappa > 1.342$ the only solutions with $A_1 = O(\epsilon)$ have $h = O(\epsilon)$, while for $\kappa < 1.342$ there are also solutions with $A_1 = O(\epsilon)$, $h \gg \epsilon$.

A similar procedure was carried out for $\kappa < \frac{1}{2}$, $A_2 < 0$. In this case, it was found that the bifurcation curve turns around and returns to the small amplitude state with a value of κ lying between 0.170 and 0.160. As will shortly be explained, this result is consistent with the 2→3 bifurcation locus springing from $\kappa = \frac{1}{6}$.

Figures 1 and 2 show the approximate bifurcation curve, at which a pure wave of degree 2 may bifurcate by the addition of subharmonic and odd superharmonic components, obtained in the way just described. In Fig. 1, the locus is plotted in the κ, A_2 plane. Figure 2 shows the results in the $\kappa, h/\lambda$ plane.

It is only for small amplitude waves that it is meaningful to talk of a (M, N) combination wave. When bifurcation occurs at finite amplitude, many Fourier

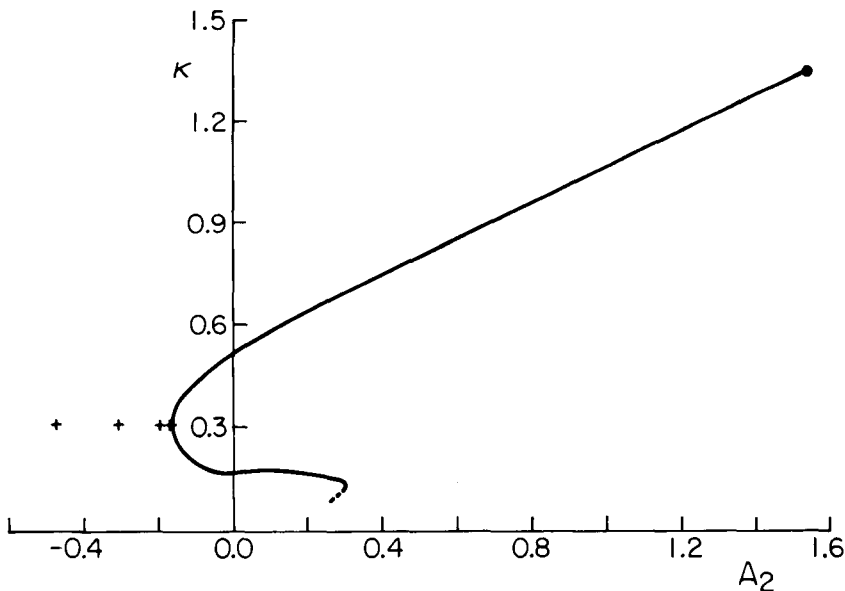


Figure 1. Sketch of the 2→1 and 2→3 bifurcation line in the κ, A_2 plane. The dot shows the wave of maximum height. The dashed line indicates that the line continues. + signs represent the solutions plotted in Fig. 3.

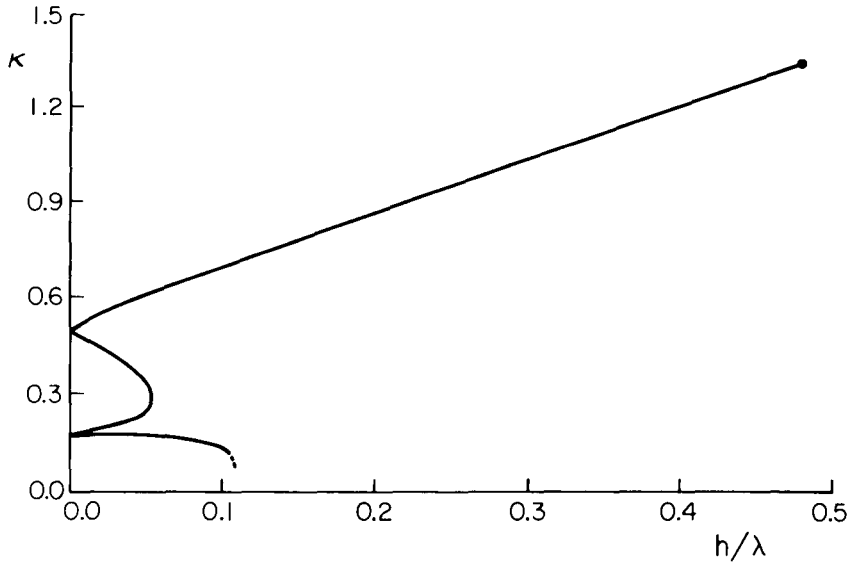


Figure 2. Sketch of the 2→1 and 2→3 bifurcation line in the $\kappa, h/\lambda$ plane. In this case, $\kappa = \pi^2 T / g \lambda^2$.

components are introduced. The combination waves which exist only outside the $A_2 < 0$ bubble in Fig. 1 are analytic continuations of one another as the bifurcation locus is traversed from $\kappa = \frac{1}{2}$ to $\kappa = \frac{1}{6}$. For $\kappa \neq \frac{1}{2}$, $A_3/A_1 \ll 1$, and for $\kappa \neq \frac{1}{6}$, $A_1/A_3 \ll 1$. Thus the return of the bifurcation locus to the κ -axis is consistent with the 2→3 bifurcation curve coming from $\kappa = \frac{1}{6}$.

As follows from the results of I, Sec. 6, the 2→3 bifurcation locus for $0 < \kappa - \frac{1}{6} \ll 1$ is the parabola

$$A_2 = \pm \left\{ \frac{3}{2} \left(\kappa - \frac{1}{6} \right) \right\}^{1/2}, \quad \text{or} \quad \left(\frac{h}{\lambda} \right)^2 = \frac{3}{2\pi^2} \left(\kappa - \frac{1}{6} \right). \quad (3.3)$$

The continuation of the bifurcation locus across $\varepsilon = 0$ at $\kappa = \frac{1}{6}$ initially follows Eq. (3.3), but as ε increases the curvature changes and the locus turns down in κ , as seen in Figs. 1 and 2. Above $\kappa = \frac{1}{8}$, we can speak of this line as being the 2→3 bifurcation line. The reason is that if we continue pure waves of degree 2 from infinitesimal to finite amplitude, keeping κ constant and $\frac{1}{8} < \kappa < \frac{1}{6}$, we obtain the same solutions as the ones found following the bifurcation locus. These waves have $A_4 < 0$. For κ near but less than $\frac{1}{8}$, the continuation of an infinitesimal wave of degree 2 to maximum amplitude with κ constant does not have any critical points but has $A_4 > 0$. The behavior of pure waves of degree 2 near $\kappa = \frac{1}{8}$ is the same as that of pure waves of degree 1 near $\kappa = \frac{1}{2}$ (see I Secs. 3 and 4). Therefore, the finite amplitude bifurcation locus for $\kappa < \frac{1}{8}$ describes the sub-harmonic bifurcation of a combination (4, 2) wave. In the κ, A_2 plane the locus

eventually returns to the κ -axis at about $\kappa=0.062$, but the wave has nonzero amplitude when this occurs and the crossing is not related to the behavior near singular points described in I.

The uncertainty in the values of κ , A_2 and h/λ for the curves shown in figures 1 and 2 is about 0.01 for κ and about the same for A_2 and h/λ when $A_2 > 0$, and about 0.003 for A_2 and h/λ when $A_2 < 0$.

The bifurcation point was determined more exactly at a few points on the bifurcation curve, and it was verified that the bifurcation conditions were satisfied. For $\kappa=0.3$, the pure wave of degree 2 bifurcates at $A_2 = -0.158$. The combination wave originating at this value was continued in A_2 until it reached its maximum height, with an enclosed bubble, at $A_2 = -0.48$, $A_1 = 0.34$, $h/\lambda = 0.27$. Plots of the profiles for this solution branch are shown in Fig. 3. Profiles of combination waves emanating from $A_2 = \pm 0.032$, continued in κ , were plotted in I, Fig. 3. These waves start to resemble pure waves of degree 1 as κ moves away from the bifurcation curve.

Most of the calculations were done using 64 Fourier coefficients. The Newton iteration converged quadratically, and 3 or 4 iterations were sufficient to reduce the residuals to $O(10^{-12})$. Each solution required less than 0.5 sec on the CDC STAR 100 computer. Some of the higher amplitude waves were recalculated using 128 Fourier coefficients. Then the computing time per solution was about 1.5 sec. In both cases all the last coefficients were $O(10^{-12})$ and the solutions agreed to at least 8 significant figures.

It is noteworthy that Choi [4] observed experimentally a doubling of wavelength like that predicted by our bifurcation analysis for capillary waves produced by wind blowing over water in a wind-water tunnel. A wind of speed 5 m/sec initially produced waves of frequency that stayed constant at 16 Hz, until after a certain fetch the frequency appeared to drop to about 9 Hz. The value of κ corresponding to Choi's experiment is 0.23 (with $T=72$ dynes/cm). Our results indicate that bifurcation is then possible at $A_2 = -0.14$ or $h=0.8$ mm. Unfortunately, Choi does not give the waveheight at which the dominant frequency changed from 16 to 9 Hz, but we roughly estimated it to be $h=1.7$ mm. The quantitative agreement is poor, but the effects of wind and shear in the water are probably significant. The observed wave speed is about 6 cm/sec greater than that given by the linear dispersion relation.

4. The finite amplitude $M \leftrightarrow N$ bifurcation with $N > \frac{1}{2}M$

As examples, we followed the $3 \rightarrow 2$, the $5 \rightarrow 4$ and the $5 \rightarrow 3$ bifurcation lines. These curves were found in the same approximate way as the $2 \rightarrow 1$ line.

For the $3 \rightarrow 2$ bifurcation we start with κ just less than $\frac{1}{6}$ and a pure 3 wave of small amplitude, and determine, by changing the parameters, where the determinant of the Jacobian changes sign. This bifurcation line also turns back, at about $A_3=0.14$, $\kappa=0.11$, and tends to the κ -axis between 0.075 and 0.087. For small amplitude waves the $3 \rightarrow 4$ bifurcation starts at $\kappa = \frac{1}{12}$. It therefore appears that the $3 \rightarrow 2$ and $3 \rightarrow 4$ bifurcation lines are different ends of the same line, and the (3, 2) and the (3, 4) combination waves are analytic continuations of one

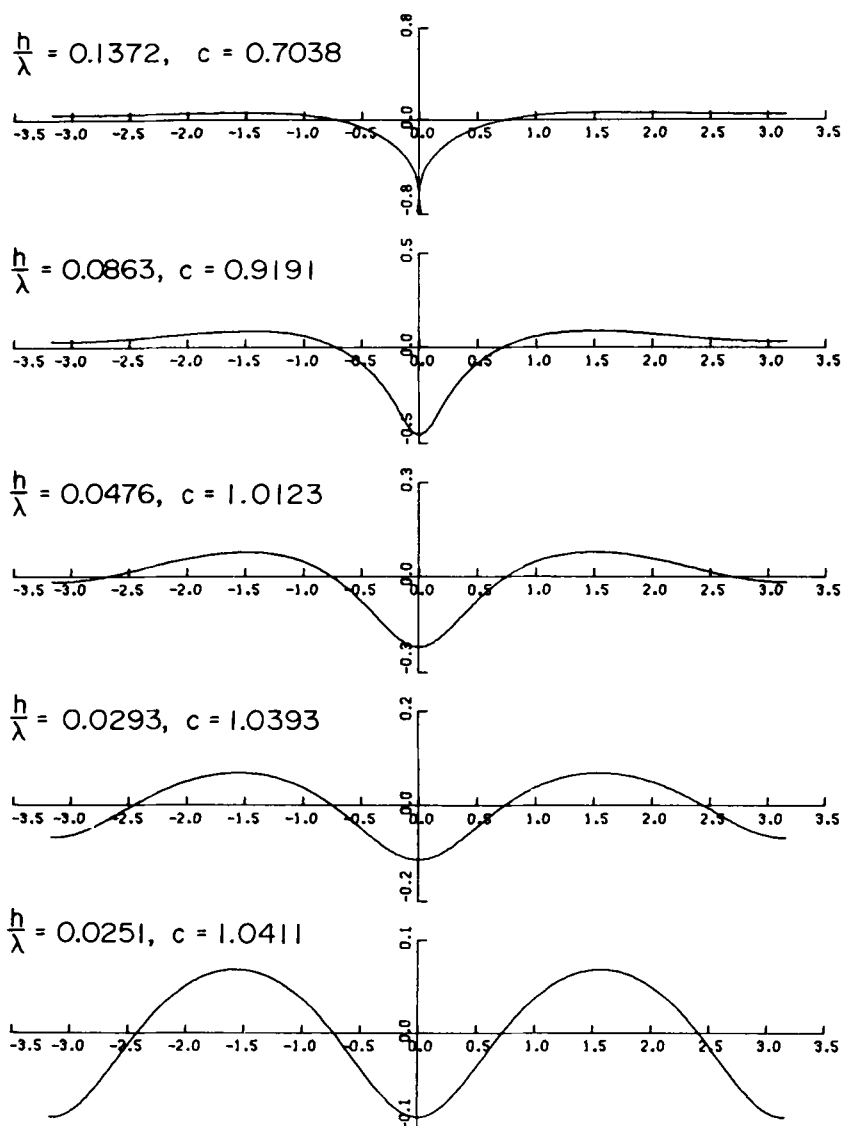


Figure 3. Profiles of (2, 1) combination waves for $\kappa = 0.3$. The lowest profile corresponds to just after the bifurcation point, and the top one to the highest wave where the surface encloses a bubble. The y origin is at the mean water level.

another. The step sizes used in finding the changes of sign of the Jacobian were at most $|\Delta\kappa| = 0.012$, $|\Delta A_3| = 0.01$. Figure 4 is a sketch of this bifurcation line. It is symmetric with respect to the κ -axis. The maximum error in the curves is of the order indicated.

The 5 \rightarrow 4 bifurcation line was followed in the same way, determining the changes of sign of the Jacobian for a pure 5 wave. In the κ, A_5 plane, this line

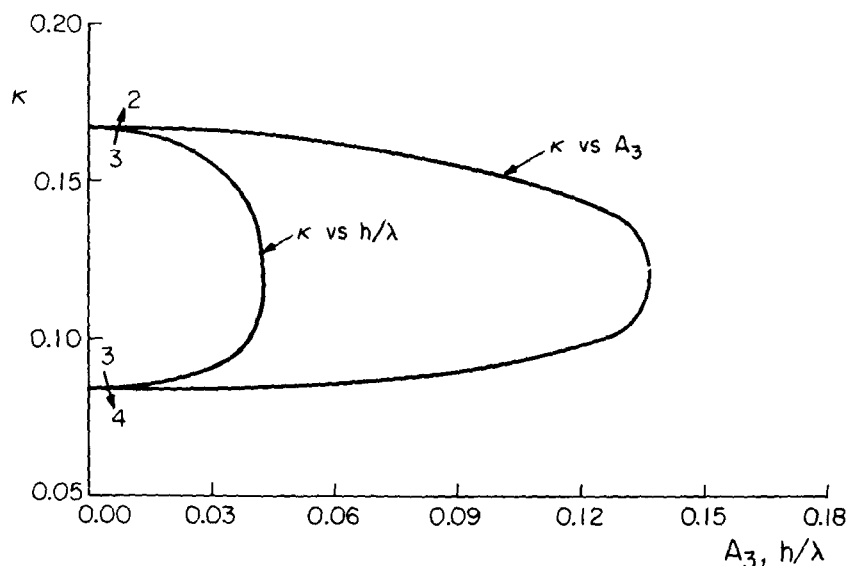


Figure 4. Sketch of the 3→2 and 3→4 bifurcation line, plotted as κ versus A_3 and κ versus h/λ .

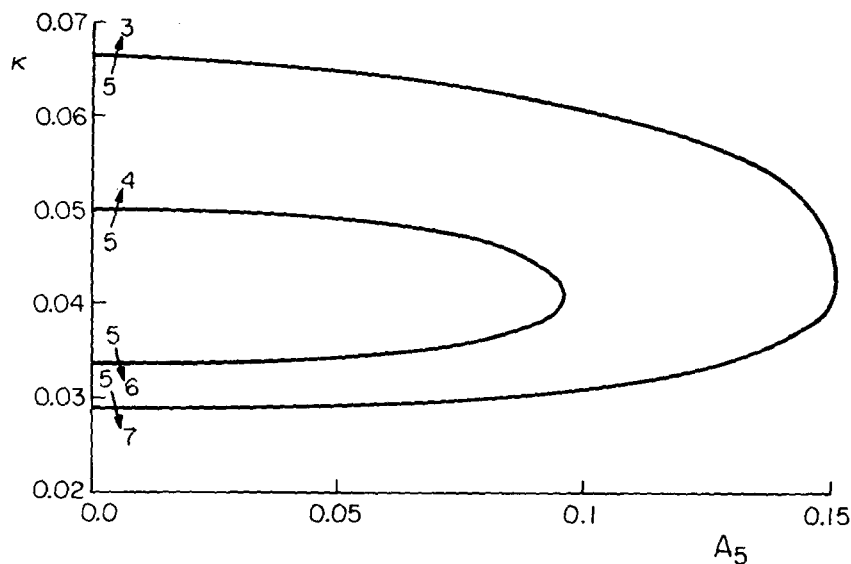


Figure 5. Sketch of the 5→3, 5→4, 5→6 and 5→7 bifurcation lines in the κ, A_5 plane.

turns back and returns to the κ -axis as the 5→6 line; the same behavior occurs for the 5→3 line, which joins onto the 5→7 line. Both lines are symmetrical about the κ -axis. The step sizes in determining these lines were $|\Delta\kappa|=0.001$ and $|\Delta A_5|=0.01$. Figure 5 shows sketches of the curves. The (5, 4) and the (5, 6) combination waves are analytic continuations of each other, as are also the (5, 3) and the (5, 7) waves.

Since all the waves that we calculate are symmetric about $\zeta = \pi$, each wave displaced horizontally by a distance $\frac{1}{2}L$ is also a solution of the system of equations for the A_n . Thus if the set $\{A_n\}$ constitutes a solution, so does the set $\{(-1)^n A_n\}$. It follows that the bifurcation loci for pure waves of odd degree N are symmetrical about the κ -axis in the κ, A_N plane. This is not necessarily true for pure waves of even degree, and it was shown in Sec. 3 that the $2 \rightarrow 3$ bifurcation locus is not symmetrical. However, it was found that the $4 \rightarrow 3$ and $4 \rightarrow 5$ bifurcation lines join up and are symmetric.

All these calculations employed 128 Fourier coefficients, the computing time for each iteration being about 1.5 seconds on the CDC STAR 100. The number of iterations depended on the initial guess, but convergence was quadratic and typically 3 or 4 iterations were sufficient to reduce the residuals to $O(10^{-12})$.

5. The $1 \rightarrow M$ limit line

As shown in I, the behavior of small pure waves of degree 1 near $\kappa = 1/M$ is a special kind. For $M \geq 4$, a pure 1 wave continued in κ , with A_1 kept constant, turns as $\kappa \rightarrow 1/M$ into a combination wave in which A_1 and A_M are of the same order. If $\kappa \rightarrow 1/M$ from above, the solution branch has a limit point in κ and turns back, with the magnitude of A_M increasing. If we start with a pure 1 wave and $\kappa < 1/M$, and then increase κ , then there is no limit point, but A_M increases rapidly as $\kappa \rightarrow 1/M$. This means that pure 1 waves on different sides of $\kappa = 1/M$ are not analytic continuations of one another.

As an example, an initially pure wave of degree 1 with $A_1 = 0.05$, and 128 Fourier coefficients retained, was continued down from $\kappa = 0.22$ to $\kappa = 0.2011$, where a limit point was encountered, and then on the second branch to $\kappa = 0.325$. At this point the surface of the wave crosses itself, with $A_1 = 0.05$ and $A_5 = -1.59$. The solution looks almost like a pure 5 wave, but the crests are of slightly different height and only two troughs enclose a bubble. The calculation was repeated, keeping $A_1 = 0.1$ constant. Now the limit point is at $\kappa = \frac{1}{5}$, so that the line moves up with increasing A_1 in agreement with the analysis of I, Sec. 8, according to which the $1 \rightarrow 5$ limit line is

$$\kappa = \frac{1}{5} + \frac{51}{160} A_1^2. \quad (5.1)$$

Also, a pure wave of degree 1 with $A_1 = 0.05$ was continued up from $\kappa = 0.171$. Around $\kappa = 0.200$, A_5 starts growing very fast and dominates the behavior. At $\kappa = 0.325$, the wave, which looks almost like a pure 5 wave with $A_5 = 1.56$, achieves its maximum height by enclosing a bubble.

In Sec. 6 we give some additional evidence that the $1 \rightarrow 5$ limit line intersects the highest wave line. This is probably true for all $1 \rightarrow M$ limit lines, for $M \geq 4$.

These results confirm the impossibility of going continuously from a pure capillary-gravity wave to a gravity wave by letting $\kappa \rightarrow 0$. We also tested to see if a combination wave could go continuously to a gravity wave. This was done by

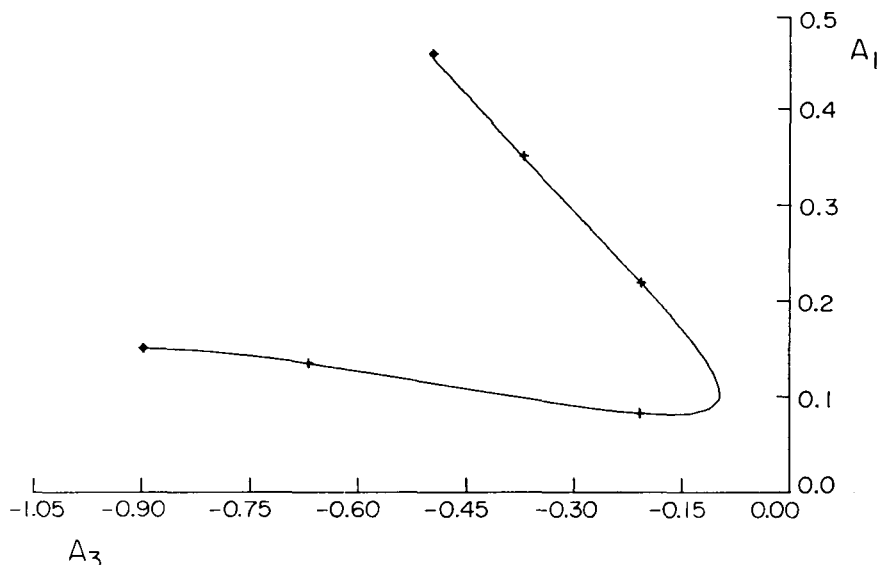


Figure 6. Plot of A_1 versus A_3 for a (1, 3) combination wave with $\kappa=0.316$. The dots represent waves of maximum height. The + signs represent the solutions of Fig. 7.

starting with a (5, 4) combination wave at $\kappa=0.05$, $A_5=0.122$, $A_4=0.179$, and continuing by decreasing κ with A_5 kept constant. This solution branch has a limit point in κ at $\kappa=0.0185$, $A_5=0.122$, $A_4=0.072$, and turns back. The value of A_5 was chosen so that the solutions were outside the $5 \rightarrow 4$, $5 \rightarrow 6$ bifurcation line. We believe that, in general, it is impossible to continue a combination wave to a gravity wave by letting $\kappa \rightarrow 0$.

The (3, 1) combination waves are also special. As shown in I, Sec. 9, for κ near $\frac{1}{3}$ there are three (1, 3) combination waves. One of them has $A_3 = O(A_1^3)$ as $A_1 \rightarrow 0$. The other two exist only for finite amplitude.

We investigated one of the latter solutions for $\kappa=0.316$. The continuation was done in A_1 . There is a limit point at $A_1=0.0818$, $A_3=-0.2667$. Continuing the solution to either side, a wave of maximum height is obtained. Figure 6 is a plot of A_1 and A_3 for this solution. On the top branch the maximum height wave has $A_1=0.453$, $A_3=-0.558$. There is also a limit point with respect to A_3 at $A_1=0.103$, $A_3=-0.202$. The other branch has a maximum height wave at $A_1=0.151$, $A_3=-0.909$. This solution has A_2 negative, and exists inside the $2 \rightarrow 1$ bifurcation line. There is no inconsistency, since the solution is not a combination (2, 1) wave.

Figure 7 shows plots of the surface profile for different solutions on this branch. The top three plots correspond to the upper branch, the fourth to the limit point in A_1 and the last two to the lower branch. A_1 decreases from the top until the fourth plot and then increases again.

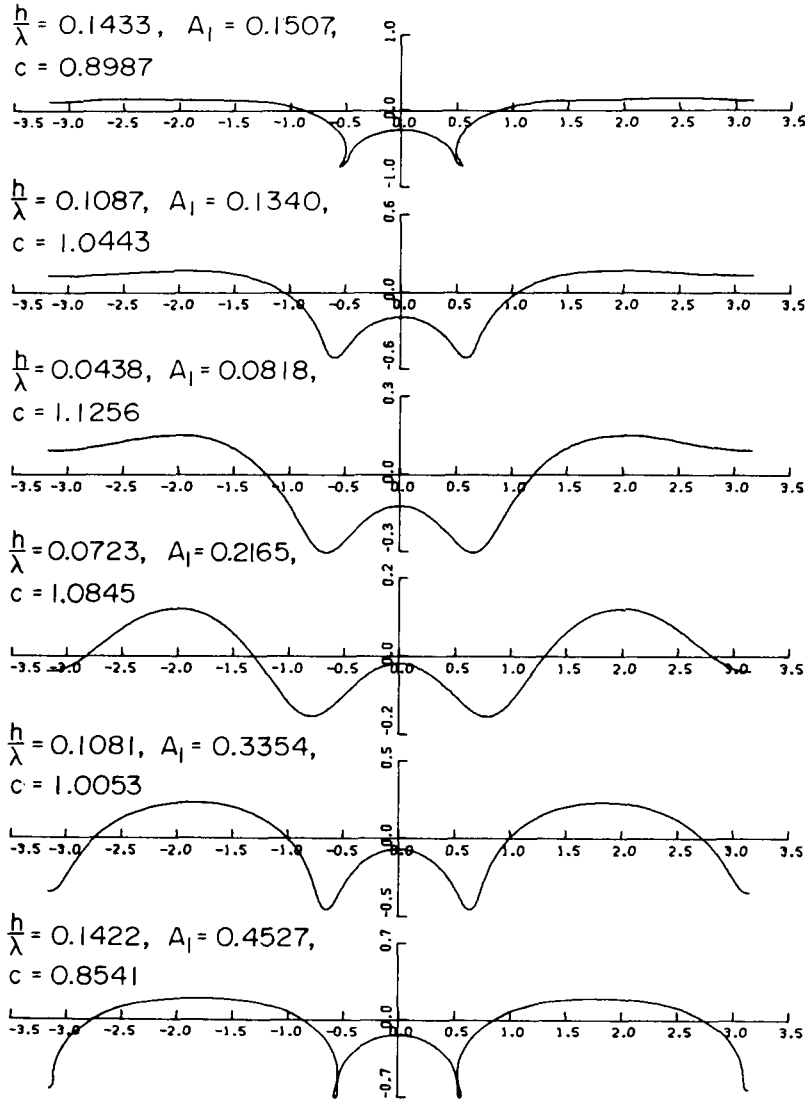


Figure 7. Profiles of (1, 3) combination waves with $\kappa=0.316$, for different points on the A_1 versus A_3 diagram of Fig. 6. The y origin is at mean water level.

6. Waves of maximum height on deep water

Gravity waves have a maximum height when the surface cusps and includes an internal angle of 120° . This occurs for the pure wave at $h/\lambda \doteq 0.1411$.

Capillary waves, as shown by Crapper [5], have a maximum height of $h/\lambda = 0.730$, but in this case the wave is limited because it encloses a bubble. For

greater heights the surface crosses itself, making the solution unphysical, even though there is no mathematical problem in the calculation of the Fourier coefficients or in determining parametric equations for the surface.

In this section we give some answers to the questions of the existence and shape of capillary-gravity waves of maximum height on deep water.

First we reproduced numerically Crapper's results with a pure wave of degree 1 up to the limiting height. We know of no simple analytical criterion to determine from a parametric Fourier representation like (2.1) if a surface crosses itself. We used some sufficient conditions for the curve to be simple and visual aids to determine when this happened. The method does not give the maximum height to great accuracy, but it turned out to be sufficient for our purposes. For pure capillary waves we found in this way the maximum height to be $h/\lambda = 0.7305$, which agrees well with Crapper's exact value.

We repeated the calculation using $\lambda = L/2$ and $\lambda = L/3$, seeking subharmonic bifurcations. None were found. If we apply the intuitive argument that bifurcation occurs when two different waves move with the same speed, we do not expect any bifurcations, since the speed decreases monotonically as the height increases. Also the $2 \rightarrow 1$ bifurcation line does not intersect the line $\kappa = \infty$, $\tilde{\kappa} = 1$.

Waves of greatest height were found in two different ways. The first method was to take Crapper's limiting solution and, by decreasing κ and then changing the amplitude, obtain waves of maximum height for different values of κ . With this method of continuation, it was possible to calculate waves with κ down to about 0.04, where the numerical solution started to become inconsistent because the higher coefficients did not remain small. We were working with 128 harmonics. Increasing this number permitted us to go to lower values of κ , but it was found that the higher order coefficients quickly grew more and more important as κ decreased. A_2 , which is positive for capillary waves, changes sign as κ decreases at about $\kappa = 1.95$ and stays negative afterwards. All the waves of greatest height calculated in this way look alike; they all enclose a single bubble and are all smooth. But as κ decreases, the bubble gets smaller and the change of slope faster. Figure 8 shows the profiles for these waves for $\kappa = \infty$, 2.333, 0.666, 0.250 and 0.042.

The second way was to start with pure waves of degree 1 of small amplitude, and increase the waveheight by changing A_1 with κ kept constant. For $\kappa > \frac{1}{2}$ the waves of greatest height are the same as those obtained by the first method of continuation. But for $\kappa < \frac{1}{2}$, the highest waves found in this way are multibubbled. The number of bubbles depends on the value of κ . For $1/(N+1) < \kappa < 1/N$, with $N \geq 2$ integer, the highest waves have N crests of different height and enclose N bubbles, not all completely closed. For example, for $\kappa = 0.493$, 0.429 and 0.370, the highest waves enclose two bubbles; for $\kappa = 0.316$ and 0.266, three bubbles exist, with only the middle one completely closed; for $\kappa = 0.220$, four bubbles exist, with two closed; for $\kappa = 0.190$, five bubbles exist, with only the middle one closed; and for $\kappa = 0.163$, six bubbles exist. Figure 9 shows the wave profiles of waves of almost maximum height for $\kappa = 0.493$, 0.316, 0.220, 0.190 and 0.163.

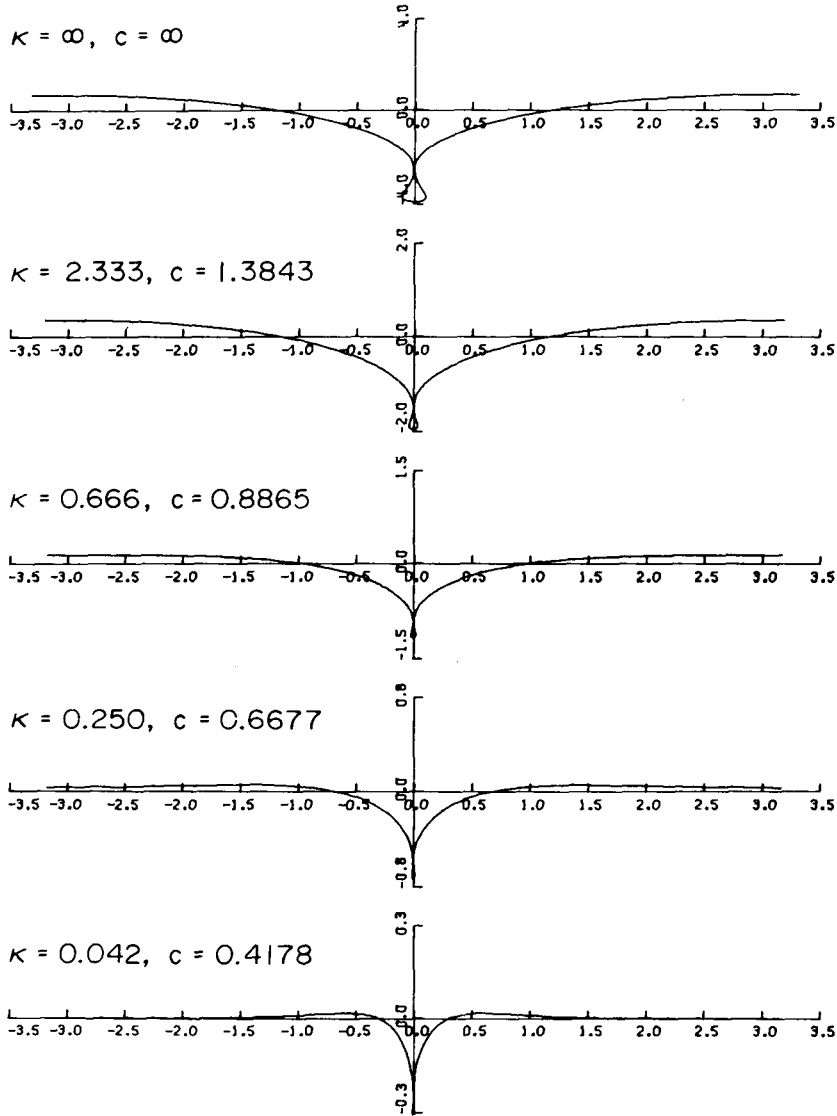


Figure 8. Profiles of waves of maximum height for $\kappa = \infty, 2.333, 0.666, 0.250$ and 0.042 . These waves are analytic continuation of Crapper's limiting solution. Origin is at mean water level.

Figure 10 shows the change of form of a pure wave of degree 1 from infinitesimal to maximum height for $\kappa = 0.190$.

For small κ , the continuation in A_1 with κ kept constant sometimes hit the $1 \rightarrow M$ limit lines in the κ, A_1 plane. The solution branch with $\kappa = 0.205$ hits the $1 \rightarrow 5$ limit line at $A_1 = 0.1192$ and turns back. After going through this limit point

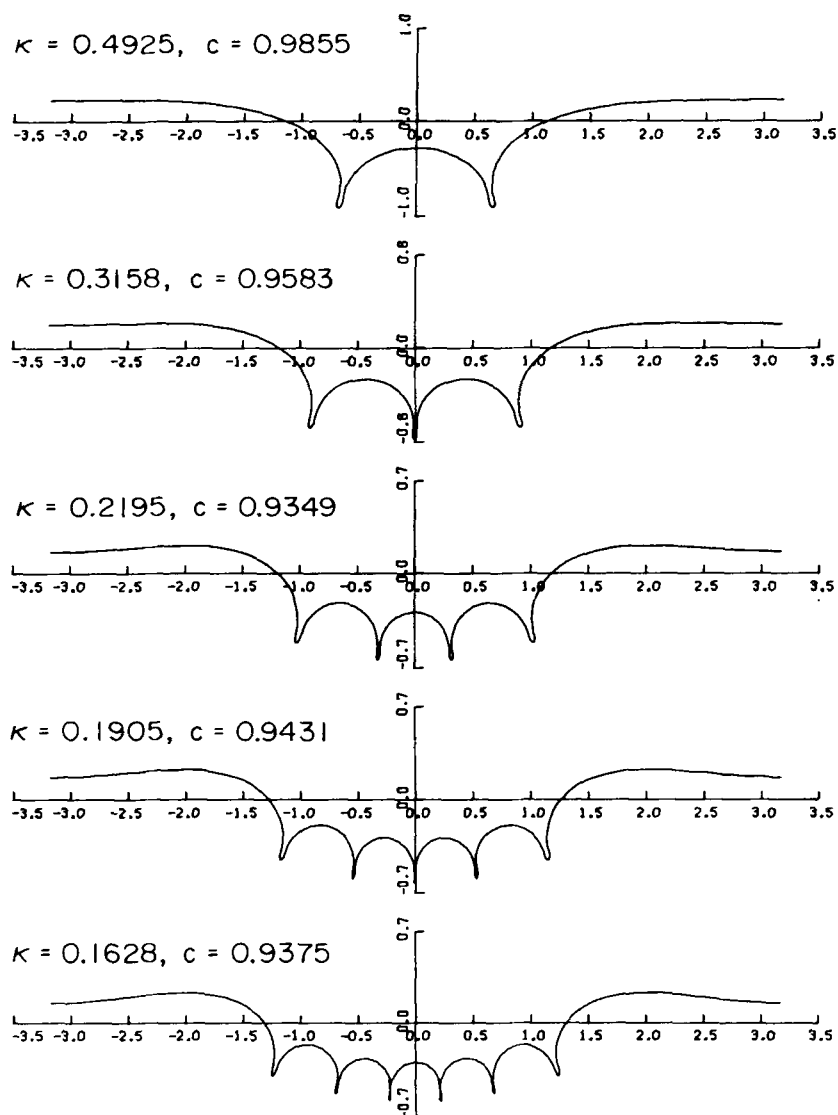


Figure 9. Profiles of waves of almost maximum height, which are the analytic continuation of pure waves of degree 1 for $\kappa = 0.493, 0.316, 0.220, 0.190$ and 0.163 . Origin is at mean water level.

the solution has 5 crests. For $\kappa = 0.176$ the solution has a limit point at about $A_1 = 0.193$ and turns back looking like a modulated 6 wave. For $\kappa = 0.149$ the solutions meet the $1 \rightarrow 7$ limit line at $A_1 = 0.15$.

For all the smaller κ , for which we used the second method of continuation, the solutions all have limit points corresponding to $1 \rightarrow M$ limit lines, before getting to the maximum. These solutions were not continued to the highest wave, because it would have required more than 128 harmonics to get a consistent solution. Since the $1 \rightarrow M$ limit lines become more concentrated as

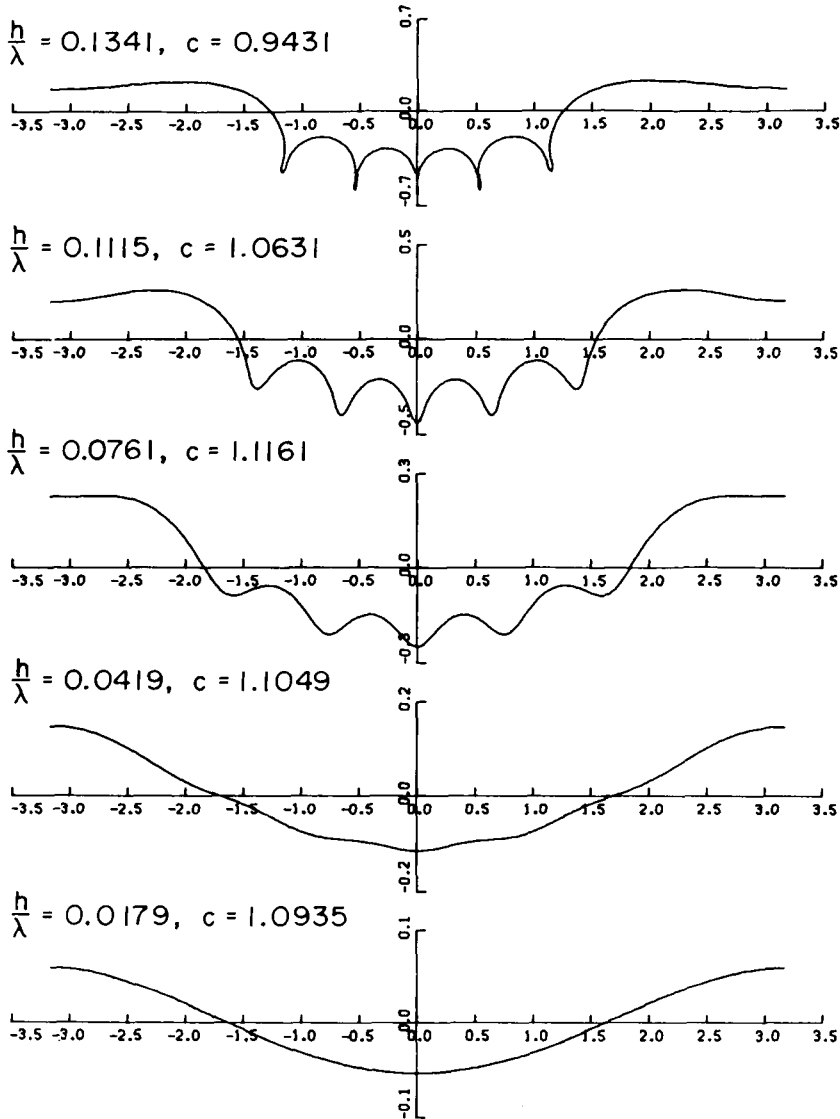


Figure 10. Profiles for different heights for a wave with $\kappa=0.190$ that started as a pure wave of degree 1 for small amplitude. Origin is at mean water level.

$\kappa \rightarrow 0$, and since they are not horizontal in the κ, A_1 plane, the continuation of the solutions using A_1 as the parameter will probably always have limit points for very small κ .

Figure 11 is a plot of $\tilde{\kappa}$ versus h/λ for maximum amplitude waves. The continuous line is for single bubbled waves which are the analytic continuation of Crapper's solution. The + signs represent multibubbled waves which are the continuation of small amplitude pure waves of degree 1, as described above.

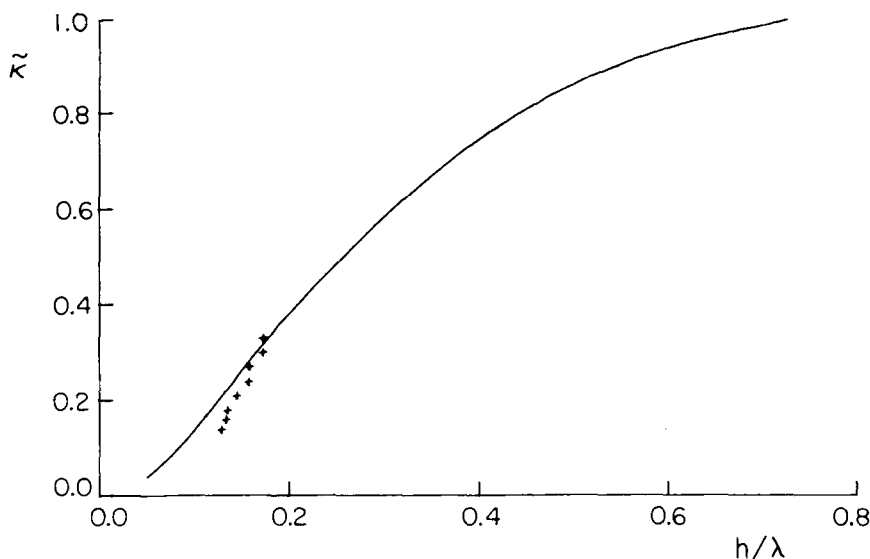


Figure 11. Plot of $\tilde{\kappa}$ versus h/λ for waves of maximum height. The continuous line corresponds to the single bubbled branch of solutions which includes Crapper's solution. The + signs correspond to multibubbled waves that started as pure waves of degree 1 for $\kappa < \frac{1}{2}$.

While the final version of this paper was being completed, we received a preprint of a paper by L. W. Schwartz and J. W. Vanden Broeck describing computations of finite amplitude capillary-gravity waves. They also note the nonuniqueness of solutions and that the waves of greatest height are determined by surface crossing, but they do not comment on the existence of bifurcation and limit lines.

Acknowledgments

We thank Control Data Corporation for providing us with time on their STAR 100 computer, without which the calculations would not have been possible. This work was supported by the Department of Energy (EY-76-S-03-0767) and the U.S. Army Research Office, Durham (DAAG 29-78-C0011).

References

1. B. M. CHEN, Ph.D. Thesis, California Institute of Technology (1979).
2. B. CHEN and P. G. SAFFMAN, Steady gravity-capillary waves on deep water—I. Weakly nonlinear waves, *Studies in Appl. Math.* 60:183–210 (1979).
3. B. CHEN and P. G. SAFFMAN, Numerical evidence for the existence of new types of gravity waves of permanent form on deep water, *Studies in Appl. Math.* 62:1–22 (1980).
4. I. CHOI, Contributions a l'étude des mécanismes physiques de la génération des ondes de capillarité-gravité a une interface air-eau, Thesis, Univ. d'Aix-Marseille II (1977).

5. G. D. CRAPPER, An exact solution for progressive capillary waves of arbitrary amplitude, *J. Fluid Mech.* 2:532–540 (1957).
6. H. B. KELLER, Numerical solution of bifurcation and nonlinear eigenvalue of problems, in *Applications of Bifurcation Theory*, Academic (1977), pp. 359–384.
7. H. LAMB, *Hydrodynamics*, Cambridge U. P. (1932).
8. A. H. NAYFEH, Triple and quintuple-dimpled wave profiles in deep water, *Phys. Fluids* 13:545–550 (1970).
9. W. J. PIERSON and P. FIFE, Some nonlinear properties of long crested periodic waves with lengths near 2.44 centimeters, *J. Geophys. Res.* 66:163–179 (1961).
10. J. R. WILTON, On ripples, *Philos. Mag.* 29:688–700 (1915).

CALIFORNIA INSTITUTE OF TECHNOLOGY

(Received February 17, 1979)